

11-23-2016

The Intestinal Copper Exporter CUA-1 Is Required for Systemic Copper Homeostasis in *Caenorhabditis elegans*

Haarin Chun

University of California at Berkeley

Anuj Kumar Sharma

University of California at Berkeley

Jaekwon Lee

University of California at Berkeley, jlee7@unl.edu

Jefferson Chan


University of California at Berkeley

Shang Jia

University of California at Berkeley

See next page for additional authors

Follow this and additional works at: <https://digitalcommons.unl.edu/biochemfacpub>

 Part of the [Biochemistry Commons](#), [Biotechnology Commons](#), and the [Other Biochemistry, Biophysics, and Structural Biology Commons](#)

Chun, Haarin; Sharma, Anuj Kumar; Lee, Jaekwon; Chan, Jefferson; Jia, Shang; and Kim, Byung-Eun, "The Intestinal Copper Exporter CUA-1 Is Required for Systemic Copper Homeostasis in *Caenorhabditis elegans*" (2016). *Biochemistry -- Faculty Publications*. 387.
<https://digitalcommons.unl.edu/biochemfacpub/387>

This Article is brought to you for free and open access by the Biochemistry, Department of at DigitalCommons@University of Nebraska - Lincoln. It has been accepted for inclusion in Biochemistry -- Faculty Publications by an authorized administrator of DigitalCommons@University of Nebraska - Lincoln.

Authors

Haarin Chun, Anuj Kumar Sharma, Jaekwon Lee, Jefferson Chan, Shang Jia, and Byung-Eun Kim

The Intestinal Copper Exporter CUA-1 Is Required for Systemic Copper Homeostasis in *Caenorhabditis elegans**[§]♦

Received for publication, September 29, 2016, and in revised form, November 15, 2016. Published, JBC Papers in Press, November 23, 2016, DOI 10.1074/jbc.M116.760876

Haarin Chun[‡], Anuj Kumar Sharma[‡], Jaekwon Lee[§], Jefferson Chan[¶], Shang Jia[¶], and Byung-Eun Kim[¶]1

From the [‡]Department of Animal and Avian Sciences, [¶]Biological Sciences Graduate Program, University of Maryland, College Park, Maryland 20742, the [§]Redox Biology Center, Department of Biochemistry, University of Nebraska, Lincoln, Nebraska 68588, and the [¶]Department of Chemistry, University of California at Berkeley, Berkeley, California 94720

Edited by F. Peter Guengerich

Copper plays key catalytic and regulatory roles in biochemical processes essential for normal growth, development, and health. Defects in copper metabolism cause Menkes and Wilson's disease, myeloneuropathy, and cardiovascular disease and are associated with other pathophysiological states. Consequently, it is critical to understand the mechanisms by which organisms control the acquisition, distribution, and utilization of copper. The intestinal enterocyte is a key regulatory point for copper absorption into the body; however, the mechanisms by which intestinal cells transport copper to maintain organismal copper homeostasis are poorly understood. Here, we identify a mechanism by which organismal copper homeostasis is maintained by intestinal copper exporter trafficking that is coordinated with extraintestinal copper levels in *Caenorhabditis elegans*. Specifically, we show that CUA-1, the *C. elegans* homolog of ATP7A/B, localizes to lysosome-like organelles (gut granules) in the intestine under copper overload conditions for copper detoxification, whereas copper deficiency results in a redistribution of CUA-1 to basolateral membranes for copper efflux to peripheral tissues. Worms defective in gut granule biogenesis exhibit defects in copper sequestration and increased susceptibility to toxic copper levels. Interestingly, however, a splice isoform CUA-1.2 that lacks a portion of the N-terminal domain is targeted constitutively to the basolateral membrane irrespective of dietary copper concentration. Our studies establish that CUA-1 is a key intestinal copper exporter and that its trafficking is regulated to maintain systemic copper homeostasis. *C. elegans* could therefore be exploited as a whole-animal model system to study regulation of intra- and intercellular copper trafficking pathways.

Copper is essential for catalytic and regulatory functions in a wide range of biochemical reactions involved in mitochondrial respiration, connective tissue formation, and iron metabolism

(1, 2). Copper deficiency is associated with pathologies that include anemia, neutropenia, and cardiomyopathy (1, 3). Additionally, if its homeostasis is not properly regulated, copper can be extremely toxic due to its stimulation of free radical production. Organisms finely tune copper homeostasis through a combination of absorption, distribution, and efflux in multiple tissues. In many species, a key aspect of copper homeostasis is facilitated by membrane-bound copper efflux pumps. Mammals have two primary copper exporters that are structurally related, ATP7A and ATP7B P-type ATPases. In tissue culture models, both of these proteins deliver copper to the lumen of the secretory machinery for incorporation into various copper-dependent enzymes at basal or low intracellular copper concentrations. At elevated cellular copper levels, ATP7A traffics to the plasma membrane to remove excess copper from cells, and ATP7B relocates to the plasma membrane and endosomes to excrete copper (2, 4). In humans, mutations in the genes encoding ATP7A and ATP7B result in severe systemic copper deficiency (Menkes disease) and hepatic/neuronal hyperaccumulation of copper (Wilson's disease), respectively (1). However, to date, copper-responsive steady-state distributions of ATP7A/B have been studied predominantly at the cellular level in tissue culture models, and regulation of their trafficking by dietary copper has not yet been thoroughly elucidated within an intact animal model (4–6).

Although the optically transparent roundworm *Caenorhabditis elegans* has emerged as a highly amenable model of micronutrient metabolism (7–9), the *C. elegans* model system has been relatively unexploited for questions related to copper homeostasis, despite the fact that these worms have a defined and highly versatile intestinal capacity for nutrient absorption (10–12). For these reasons, we utilized *C. elegans*, which has been widely used in the study of the metabolism of other metals, including iron, heme, and zinc (8, 13–17). Although mammals have two copper exporters, serving complementary functions in different tissues such as the gut and liver, lower metazoans (including nematodes (*C. elegans*) and insects (*Drosophila melanogaster*)) have only a single homolog of ATP7A/B (2, 18, 19). The protein product of *C. elegans* *cua-1* shares very high sequence similarity with human ATP7A/B. Previous studies have used yeast to demonstrate that *cua-1* has copper efflux functions, as the gene encoding *C. elegans* CUA-1 could rescue a yeast strain lacking the *CCC2* gene, which encodes a functional counterpart (20). In worms, transcriptional reporters

* This work was supported in part by National Institutes of Health Grants DK079209 (to J. L.) and GM79465 (to S. J. and J. C.), Nebraska Redox Biology Center Grant P30GM103335 (to J. L.), and by the Human Frontiers Science Program (to J. C.). The authors declare that they have no conflicts of interest with the contents of this article. The content is solely the responsibility of the authors and does not necessarily represent the official views of the National Institutes of Health.

♦ This article was selected as one of our Editors' Picks.

§ This article contains supplemental Table S1 and Figs. S1–S7.

¹ To whom correspondence should be addressed. Tel.: 301-405-3977; Fax: 301-405-7980; E-mail: bekim@umd.edu.

CUA-1 Trafficking for Organismal Copper Balance

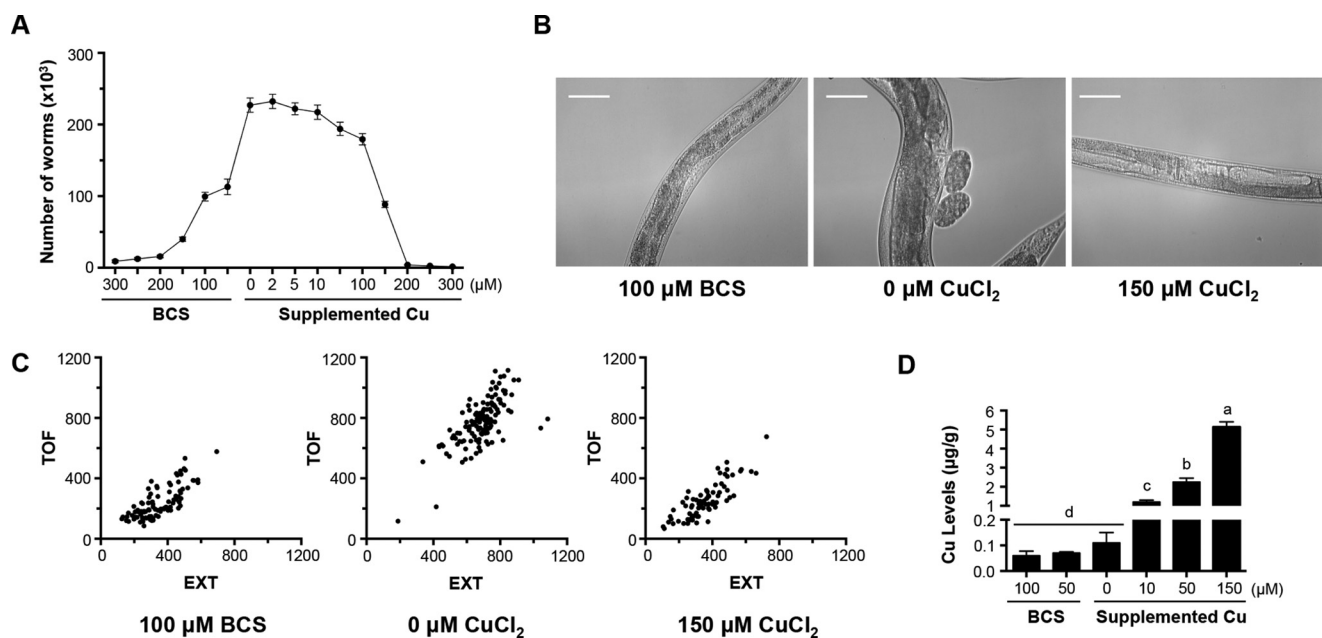


FIGURE 1. Growth of *C. elegans* is affected by dietary copper. *A*, population growth rates of wild-type N2 worms cultured in the presence of increasing amounts of CuCl₂ or BCS on NGM dishes. Fifty synchronized L1 stage worms were grown on 10-cm plates for 8 days under specified conditions and quantified by microscopy. Error bars are mean ± S.E. of three independent experiments. *B*, synchronized L1 worms were cultured on plates supplemented with different levels of copper or BCS for 3 days. Representative differential interference contrast images of worms 3 days post-hatch are shown. Scale bar, 50 μm. *C*, synchronized L1 larvae grown on NGM plates for 2.5 days were sorted by a COPAS Biosort. Time of flight (TOF) and extinction (EXT) denote the length and optical density (width) of worms, respectively. *D*, total copper levels of L4 stage wild-type worms grown on agar plates with varying levels of dietary copper were determined by ICP-MS. Error bars indicate mean ± S.E. of 3–6 independent experiments, and different letters indicate significantly different means ($p < 0.05$) (one-way ANOVA, Tukey's post hoc test) (see also supplemental Fig. S1, A and B).

have been used to detect *cua-1* expression in several tissues, including the intestine. An essential role for *cua-1* for copper transport in *C. elegans* has been suggested, as deletion of *cua-1* results in embryonic lethality (18, 21). However, how CUA-1 in the intestine responds to systemic copper status is not understood, and its intracellular location and copper responsiveness have not been determined.

Here, we report the importance of copper in *C. elegans* development and a distinct role for CUA-1 in mediating copper transport. Expression of *cua-1* specifically in the intestine is sufficient to rescue the embryonic lethal phenotype of the *cua-1* mutant. A CUA-1 translational fusion protein primarily localizes to the basolateral membrane of the intestine under basal and copper-deficient conditions but redistributes to lysosome-related organelles (gut granules) in response to elevated copper levels in the diet. Moreover, copper injection into the pseudocoelom, a fluid-filled body cavity between the intestine and the body wall, leads to a significant endosomal re-localization of intestinal CUA-1 even in dietary copper-deprived worms. Our studies show that intestinal CUA-1 is a key component regulating copper supply and detoxification to maintain systemic copper homeostasis in the intact animal.

Results

Dietary Copper Levels Affect Worm Growth—Living organisms have an optimal range of copper concentrations, and dietary excess or deficiency of copper causes various diseases and developmental defects in a broad range of organisms (1, 2). To determine the dietary copper requirements of *C. elegans* grown

on NGM² plates fed with the *Escherichia coli* strain OP50, we followed worm growth over 8 days under copper restriction using the copper(I)-specific chelator bathocuproinedisulfonic acid (BCS) or with copper supplementation using CuCl₂. Worm growth showed a biphasic curve over dietary copper levels (Fig. 1A). *C. elegans* displayed maximal growth in the low micromolar range of supplemental copper and impaired growth at either end of the copper spectrum, 100 μM BCS and 150 μM copper, with smaller brood size and delayed development. Large amounts of copper (≥200 μM) resulted in growth arrest at the L3 stage, likely due to copper toxicity. Monitoring of animal development revealed that at optimal copper (~2 μM), worms became gravid adults in 3 days, whereas most animals grown at high or low copper conditions only reached the L3 to young adult stage at this time point (Fig. 1B).

To quantify the effect of dietary copper on each animal within a mixed population, we used a COPAS Biosort instrument. Animal development was significantly delayed by supplementation of high doses of either copper or BCS (Fig. 1C). To complement the analysis of how dietary copper influences worm growth, whole-animal copper content was measured using inductively coupled plasma-mass spectrometry (ICP-MS). Worms cultured with high copper (150 μM) had only a 5-fold increase in copper content as compared with animals grown on 10 μM copper supplementation, whereas the relative

²The abbreviations used are: NGM, nematode growth medium; MEF, mouse embryonic fibroblast; BCS, bathocuproinedisulfonic acid; ICP-MS, inductively coupled plasma MS; CCS, copper chaperone for superoxide dismutase; ANOVA, analysis of variance; qRT, quantitative RT.

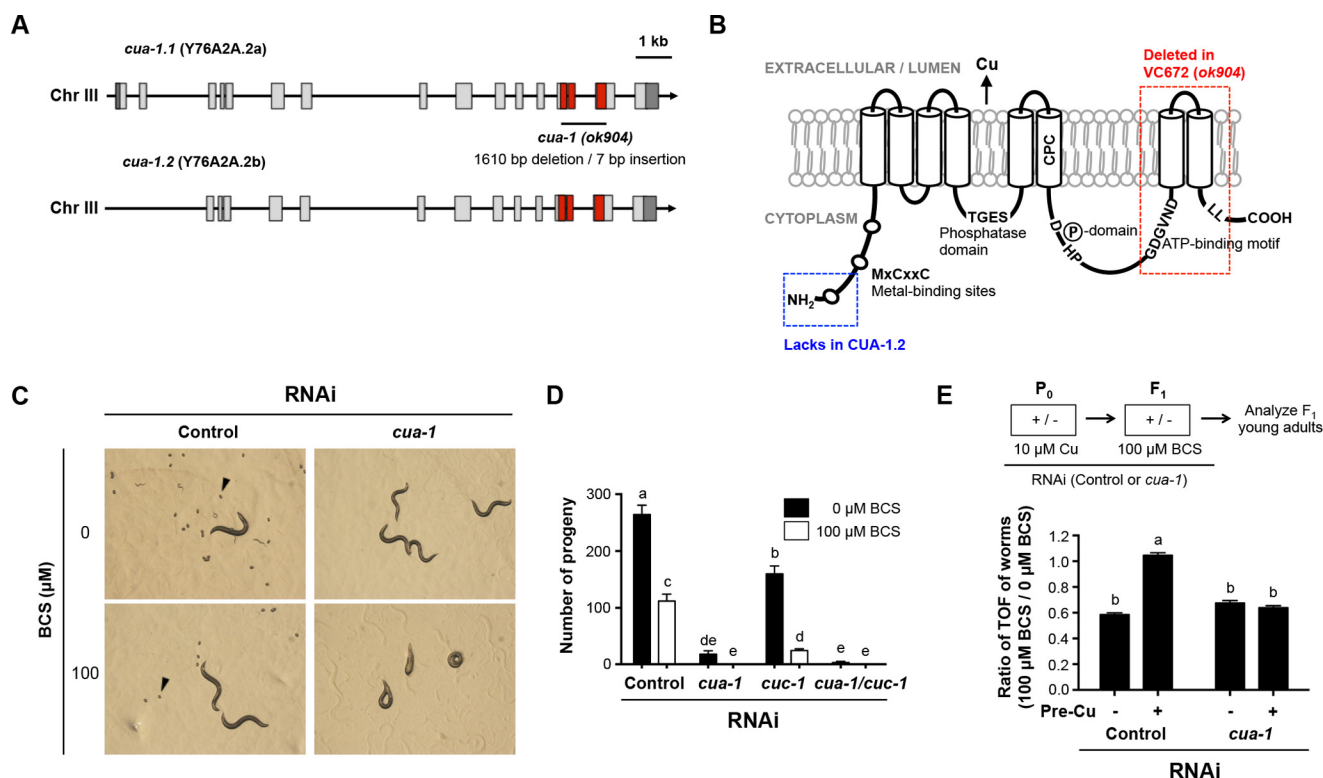


FIGURE 2. *cua-1* is required for larval development under low copper conditions. *A*, schematic diagram of the *C. elegans* *cua-1* gene. The straight line indicates genomic DNA on *C. elegans* chromosome III. The *cua-1.2* transcript lacks the first two exons as compared with the full-length *cua-1.1* isoform. *B*, predicted CUA-1 membrane topology. Domains required for copper transport activity, including metal-binding sites, a phosphatase domain, a CPC motif (Cys-Pro-Cys), a phosphorylation motif, and a dileucine-based sorting signal present in human ATP7A/B are highly conserved in CUA-1. The genomic regions of *cua-1* that are deleted in the *ok904* allele are shown in the red box, and the N-terminal truncation in CUA-1.2 is shown in the blue box. *C*, L1 worms were exposed to RNAi for 4 days with or without 100 μM BCS treatment; representative microscope images are shown. Note that *cua-1* RNAi used in this study targets the last two exons of both *cua-1.1* and *cua-1.2*. Arrowhead indicates eggs that have already been laid. *D*, L4 larval stage worms grown under varying RNAi and BCS conditions were picked to individual plates, allowed to lay eggs, and transferred to fresh plates every 24 h for 3 days. Eggs were counted for each brood treatment, and progeny number for each brood was determined as the sum of total eggs and larvae, $n = 5$ (two-way ANOVA, Tukey's post hoc test). Error bars represent average \pm S.E. Values with different letters are significantly different from each other ($p < 0.05$). *E*, wild-type P_0 animals were precultured for 3 days on NGM plates containing 0 or 10 μM supplemental copper, and synchronized F_1 progeny were cultured from the L1 stage for 2 days on plates with the indicated levels of BCS. TOF was determined by a COPAS Biosort. Lower values indicate more severely retarded growth of worms under dietary copper deficient conditions as compared with controls (no BCS supplementation). Three independent experiments were performed with ~ 200 worms for each sample. Error bars represent average \pm S.E., and different letters indicate significantly different means ($p < 0.05$) (two-way ANOVA, Tukey's post hoc test).

ratio of supplemental copper concentrations (15-fold) is higher, implying the existence of a homeostatic regulatory mechanism for maintaining optimal copper levels in *C. elegans* (Fig. 1D). BCS treatment resulted in $\sim 40\%$ reduction in total copper content as compared with no supplementation. No significant changes in iron and zinc content were observed in worms treated with copper or BCS (supplemental Fig. S1, A and B). Collectively, these data indicate that dietary copper levels impact growth and development within one generation in *C. elegans*.

CUA-1 Is Essential for Larval Development in *C. elegans*—Although vertebrates have two copper exporters, unicellular organisms and invertebrates have a single copper exporter, suggesting that the copper exporter gene duplication to ATP7A and ATP7B occurred following the branching off of the vertebrate phyla (supplemental Fig. S2, A and B). In worms, *cua-1* encodes a putative copper exporter (20), which shares about 45% sequence identity at the amino acid level with human ATP7A and ATP7B. Importantly, the motifs known to be essential for copper transport and protein trafficking in the human ATP7A/B are highly conserved in CUA-1 (Fig. 2B and supplemental Fig. S2B). The genomic structure of *cua-1* con-

sists of 16 exons, and it is predicted to encode two splice isoforms. The first isoform, *cua-1.1* (Y76A2A.2a), contains all exons, whereas the *cua-1.2* (Y76A2A.2b) isoform lacks the first two exons, which encode the first metal-binding domain (Fig. 2, A and B).

To ascertain the physiological function of *cua-1*, worms were analyzed for growth and developmental phenotypes after knockdown of *cua-1*. Without copper supplementation, animals treated with *cua-1* RNAi at the L1 stage became gravid adults in 4 days but failed to lay eggs. For worms grown in the presence of 100 μM BCS, treatment with *cua-1* RNAi resulted in near total lethality, whereas vector control worms only showed a delayed F_1 hatching (Fig. 2C). Together, these results indicate that *cua-1* is required for normal growth in *C. elegans*. To further explore the importance of *cua-1* in fecundity, total brood size was quantified. Regardless of RNAi conditions, addition of 100 μM BCS resulted in reduced brood sizes, indicating that dietary copper uptake is essential for normal reproduction (Fig. 2D). In mammals, cytosolic copper is delivered to either ATP7A or ATP7B by the copper chaperone ATOX1. In *C. elegans*, CUC-1 is a putative ATOX1 homolog that has been previously identified by yeast complementation assay (18).

CUA-1 Trafficking for Organismal Copper Balance

Depletion of *cua-1* or *cuc-1* by RNAi resulted in a decrease in brood size as compared with vector control RNAi (Fig. 2D). Double knockdown of *cua-1/cuc-1* led to a severe egg-laying defect, suggesting that a CUC-1/CUA-1 copper relay and transport pathway is conserved in *C. elegans*, analogous to the ATOX1-ATP7A/B pathway in mammals.

To investigate the physiological significance of maternal copper availability to progeny, RNAi against *cua-1* with either 0 or 10 μM supplemental copper was conducted for 3 days until parental animals (P_0) reached adulthood, and their synchronized L1 progeny (F_1) were cultured under identical RNAi knockdown conditions in the presence or absence of BCS for 2 days. Worms treated with *cua-1* RNAi whose parents were grown in 0 μM supplemental copper displayed delayed growth rates in the presence of BCS as compared with those treated with vector control (data not shown). When mothers were provided with 10 μM supplemental copper, the growth rate of F_1 progeny treated with control RNAi was faster than that of progeny from mothers that received no supplemental copper (Fig. 2E). However, the growth rate of the *cua-1* knockdown progeny was not strongly affected when the mothers were cultured in 10 μM supplemental copper (Fig. 2E). These results suggest that viability of embryos is both dependent upon maternal copper status and upon *cua-1* activity.

CUA-1 Expression Is Regulated by Dietary Copper—To determine whether *cua-1* is transcriptionally regulated by dietary copper, wild-type N2 worms were cultured with no supplementation, with 150 μM copper, or with 100 μM BCS, and mRNA levels were measured by quantitative real time PCR (qRT-PCR). Levels of *cua-1* mRNA were modestly elevated under copper-limited conditions compared with copper supplementations (Fig. 3A). To further analyze *cua-1* expression and localization, we generated transgenic animals expressing CUA-1::GFP translational fusions under the control of an endogenous promoter using the CUA-1.1 isoform, as this isoform is the full-length form of the CUA-1 gene. $P_{cua-1}::CUA-1.1::GFP$ transgenic animals showed similar tissue distribution patterns to the previously reported transcriptional reporter worms, which was primarily intestine, neurons, hypodermis, and pharynx (18), although the intestinal expression was concentrated mainly in the anterior of the intestine (Fig. 3B).

The strain VC672 contains a deletion in *cua-1(ok904)*, spanning exons 13–15 (Fig. 2A; supplemental Fig. S2C), which is genetically balanced due to the embryonic lethality of *cua-1* mutant worms (21, 23). The *cua-1(ok904)* deletion removes a region containing the last two transmembrane helices as well as an ATP-binding motif and a dileucine-based sorting signal (Fig. 2B). The *cua-1(ok904)* mutant is rescued with the transgene $P_{cua-1}::CUA-1.1::GFP$, indicating that the CUA-1.1::GFP translational fusion protein is functional (Fig. 3C). To further confirm whether the CUA-1.1::GFP translational fusion protein can transport copper, we exploited previously established assays in *Atp7a*^{+/+} and *Atp7a*^{-/-} mouse embryonic fibroblasts (MEFs) (24). *Atp7a*^{-/-} MEFs transiently transfected with CUA-1.1::GFP showed increased expression of copper chaperone for superoxide dismutase (CCS), indicating decreased levels of cellular copper (25, 26) as compared with *Atp7a*^{-/-} MEFs transfected with an empty vector (supplemental Fig. S3A).

Over-accumulated copper in *Atp7a*^{-/-} MEFs was rescued by ectopic expression of CUA-1.1::GFP (supplemental Fig. S3B), further indicating that CUA-1.1 can export copper. Moreover, these results demonstrate that a C-terminal GFP tag does not significantly interfere with CUA-1 function.

Unexpectedly, when transgenic worms ($P_{cua-1}::CUA-1.1::GFP$) were maintained at low copper concentrations (50 μM BCS), stronger CUA-1.1::GFP expression was observed in the hypodermis, whereas GFP expression levels were not altered in other tissues such as the intestine and neurons (Fig. 3C). Indeed, quantification of CUA-1.1::GFP by COPAS Biosort and immunoblotting assay showed significantly enhanced CUA-1.1::GFP levels under low copper conditions, suggesting that copper-dependent regulation in the hypodermal cells contributes to the overall steady-state abundance of CUA-1.1 (Fig. 3, D and E).

To determine the contribution of each tissue to the embryonic lethal phenotype of *cua-1* mutant worms, we carried out tissue-specific RNAi experiments. Mutant *rde-1* worms are resistant to RNAi, but restoring tissue-specific expression of the wild-type *rde-1* cDNA in these mutants confers RNAi sensitivity to a specific tissue (27). We depleted *cua-1* in wild-type N2, WM27 (*rde-1* mutant, RNAi insensitive), VP303 ($P_{nhx-2}::RDE-1$, intestine only RNAi), WM118 ($P_{myo-3}::RDE-1$, muscle only RNAi), and NR222 ($P_{lin-26}::RDE-1$, hypodermis only RNAi) worm strains (13). Knockdown of *cua-1* in the intestine resulted in reduced fecundity similar to that of whole-body RNAi (Fig. 3F), indicating that intestinal CUA-1 is crucial for the survival of worms. Although significant effects were not observed when *cua-1* was knocked down in muscle, depletion of *cua-1* in the hypodermis caused a severe reduction in brood size under low dietary copper conditions (Fig. 3F). Copper supplementation (10 μM) was able to rescue the reduced brood sizes phenotype caused by *cua-1* RNAi in each of these strains (Fig. 3F). These results imply a critical role of both intestinal and hypodermal CUA-1 in worm growth under copper-deficient conditions.

Intestinal Expression of *cua-1.1* Is Sufficient to Rescue the Lethal Phenotype of *cua-1(ok904)*—Given that targeted depletion of *cua-1* in the intestine caused similar phenotypes as whole-body RNAi, we examined the subcellular localization of CUA-1.1 by driving the expression of CUA-1.1::GFP from the strong constitutive intestine-specific *vha-6* promoter (28). $P_{vha-6}::CUA-1.1::GFP$ localized to basolateral membranes and to intracellular compartments, reminiscent of basolateral sorting and recycling endosomes in the *C. elegans* intestine (Fig. 4A) (29). Importantly, the embryonic lethal phenotype of *cua-1(ok904)* mutant can be rescued by intestine-specific expression of CUA-1.1::GFP (Fig. 4, B and C) suggesting that the intestine is the key site of copper regulation in *C. elegans*. These results are further corroborated by the fact that RNAi depletion of either *cuc-1* or *cua-1* in $P_{vha-6}::CUA-1.1::GFP;cua-1(ok904)$ transgenic animals grown in low copper results in a lethal phenotype that can be rescued by copper supplementation. These observations suggest that a CUC-1/CUA-1 copper delivery pathway from intestine to peripheral tissues is essential for worms under dietary copper restriction (Fig. 4, B and C). To further assess the significance of intestinal CUA-1 function

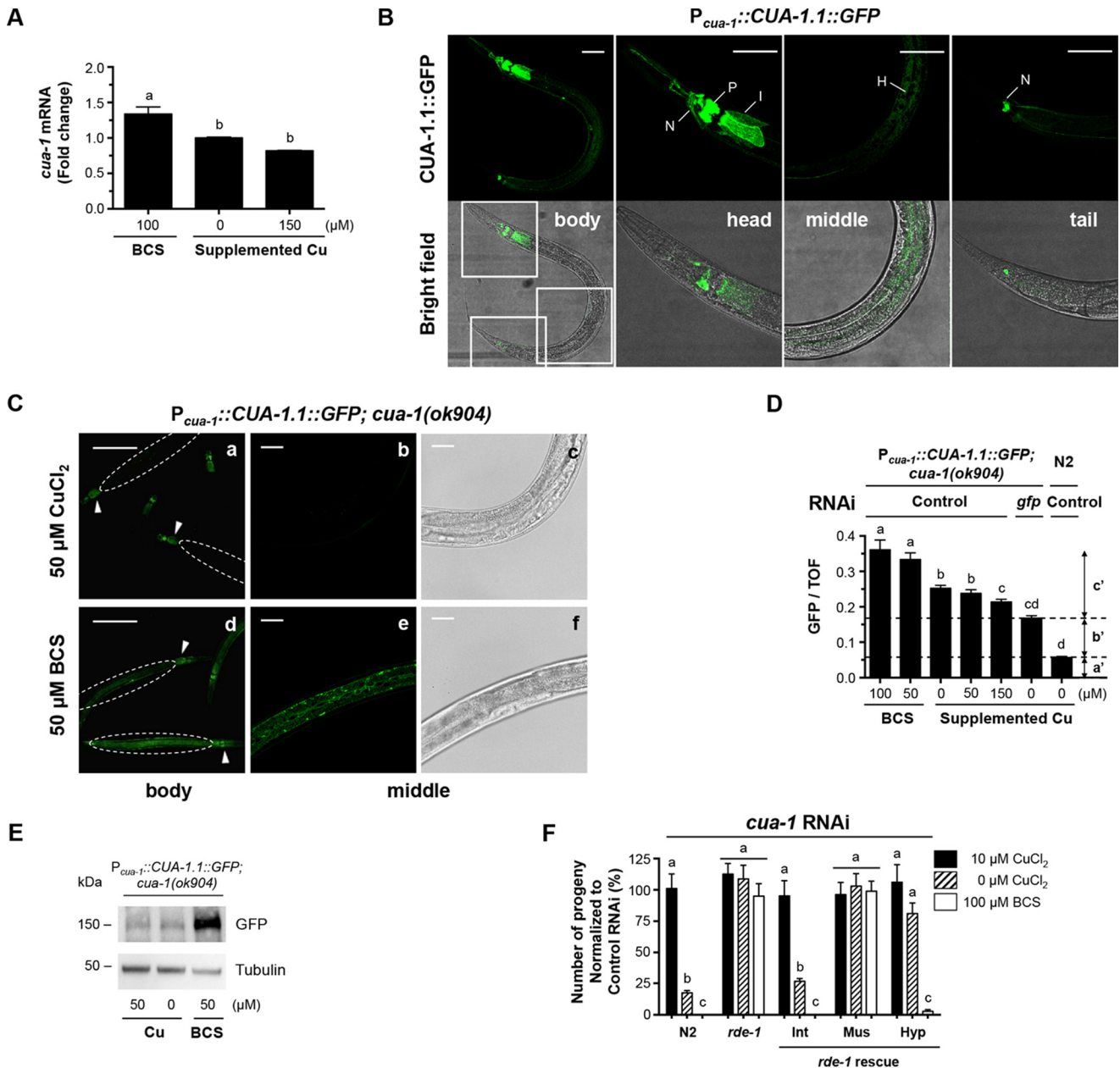


FIGURE 3. Copper deficiency induces *cua-1* in *C. elegans*. *A*, wild-type L1 worms were cultivated with no supplemental copper, 150 μ M copper, or 100 μ M BCS for 2.5 days. The relative fold changes of *cua-1* mRNA levels were determined by qRT-PCR. *Bars* indicate mean \pm S.E. of three independent experiments. Means followed by *different letters* are significantly different at $p = 0.05$ (one-way ANOVA, Tukey's post hoc test). *B*, live transgenic animals expressing a *cua-1.1* translational reporter ($P_{cua-1}::CUA-1.1::GFP::unc-54$ 3' UTR) were imaged by confocal microscopy. *I*, intestine; *N*, neurons; *P*, pharynx; *H*, hypodermis. *Scale bar*, 50 μ m. *C*, elevated CUA-1.1::GFP expression in the hypodermis by BCS supplementation was detected in transgenic animals ($P_{cua-1}::CUA-1.1::GFP::unc-54$ 3' UTR; *cua-1(ok904)*). The *arrowheads* and *dashed circles* indicate the anterior intestinal cells and hypodermis, respectively. Note that *panels b-c* and *e-f* are magnified images. *Scale bars*, 200 μ m (*panels a* and *d*) and 25 μ m (*panels b-c* and *e-f*). *D*, normalized GFP was analyzed using a COPAS Biosort. Background fluorescence and neuronal CUA-1.1::GFP fluorescence (which is refractory to RNAi knockdown), are indicated by *a'* and *b'*, respectively. As such, *c'* represents CUA-1.1::GFP expression specifically in the intestine, hypodermis, and pharynx. *Error bars* show mean \pm S.E. of a single experiment with ~ 200 worms. Groups that do not share the same letter are significantly different ($p < 0.05$) (one-way ANOVA, Tukey's post hoc test). *E*, immunoblot analysis of CUA-1.1::GFP in transgenic worms ($P_{cua-1}::CUA-1.1::GFP::unc-54$ 3' UTR; *cua-1(ok904)*). Worm lysates were subjected to SDS-PAGE followed by immunoblotting using anti-GFP and anti-tubulin antibodies. Tubulin is shown as a loading control. *F*, depletion of *cua-1* in the intestine recapitulated the reduced fecundity of whole-animal RNAi. Wild-type N2, RNAi-resistant worm strain (*rde-1*), and tissue-specific RNAi lines were cultured on RNAi dishes with indicated concentration of copper or BCS. *Int*, intestine-specific RNAi; *Mus*, muscle-specific RNAi; *Hyp*, hypodermis-specific RNAi. *Error bars* represent mean \pm S.E. Values with one different superscript letter are significantly different from each other ($p < 0.05$). $n = 3$ (two-way ANOVA, Tukey's post hoc test).

under varying copper availability, F_1 progeny of N2 wild-type, $P_{vha-6}::CUA-1.1::GFP$, and $P_{vha-6}::CUA-1.1::GFP;cua-1(ok904)$ worms derived from P_0 worms exposed to 10 μ M copper were grown to the L4/young adult stage under different dietary copper conditions and then analyzed by COPAS Biosort. Transgenic animals expressing CUA-1.1::GFP under control of the

vha-6 promoter exhibited a reduced growth phenotype when exposed to high copper and enhanced growth under copper restriction in a dose-dependent manner (Fig. 4, *C* and *D*). We attribute the copper hypersensitivity to the constitutive overexpression of CUA-1.1 in the intestine, which would lead to the export of copper into the worm body. In line with the assertion

CUA-1 Trafficking for Organismal Copper Balance

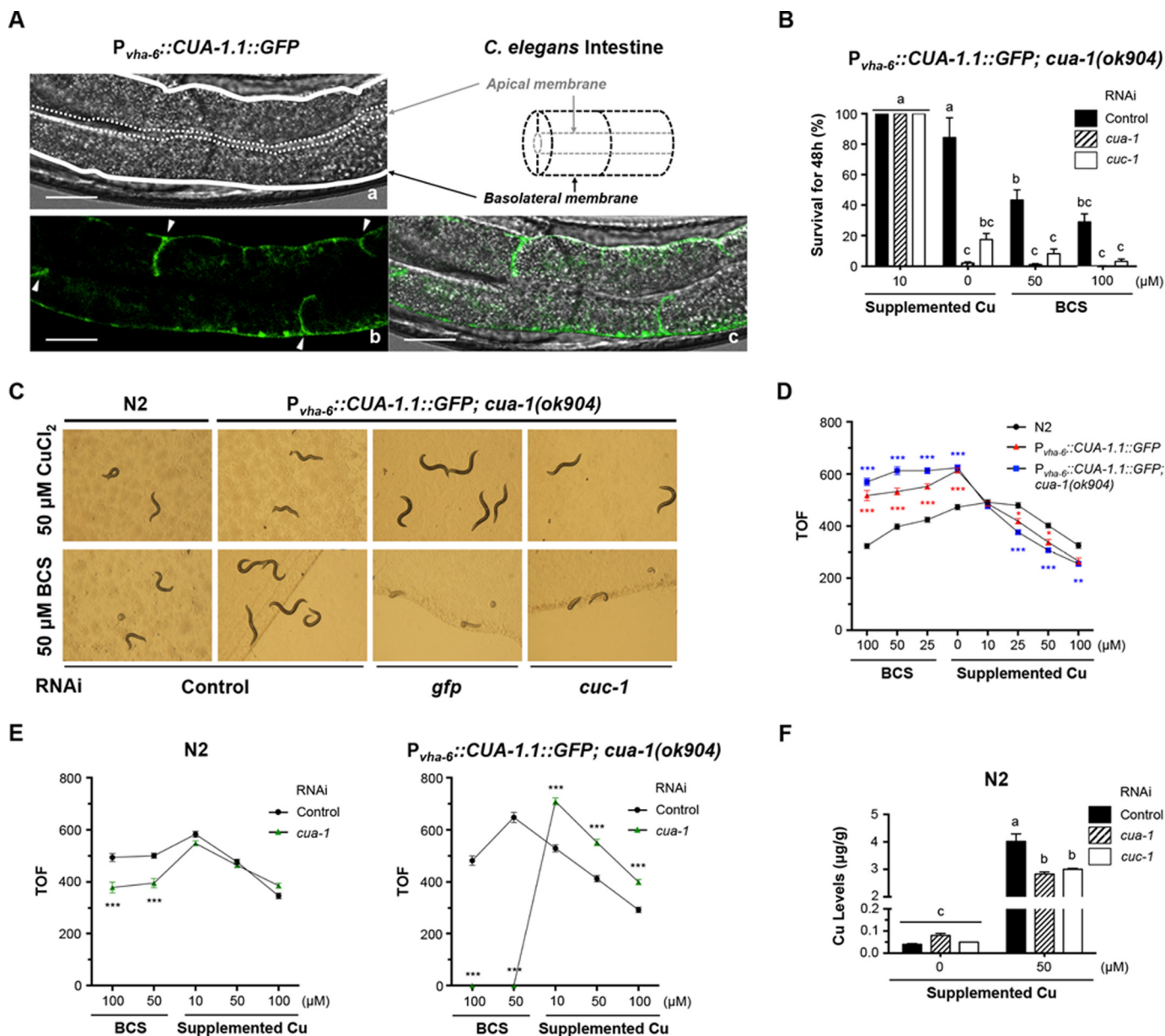


FIGURE 4. Copper export by intestinal CUA-1 is essential for survival. *A*, transgenic worms expressing a *cua-1.1* translational reporter (*P_{vha-6}::CUA-1.1::GFP::unc-54 3' UTR*) were imaged by confocal microscopy. The bright field image (*panel a*) shows the morphology of the worm intestine, and the green signal (*panel b*) shows CUA-1.1::GFP expression therein. Dotted lines indicate apical membrane; solid lines indicate basal membrane; and arrowheads indicate lateral membranes in polarized intestinal cells. Scale bar, 20 μm. *B* and *C*, survival rates (*B*) and images (*C*) of transgenic worms (*P_{vha-6}::CUA-1.1::GFP::unc-54 3' UTR;cua-1(ok904)*) cultured on RNAi plates supplemented with either copper or BCS 48 h post-hatch. Error bars indicate average \pm S.E. Means that do not share a letter are significantly different ($p < 0.05$). $n = 3$ (two-way ANOVA, Tukey's post hoc test). *D*, P₀ worms were treated with 10 μM supplemental copper on NGM plates with *E. coli* OP50. Synchronized L1 stage wild-type N2 worms and transgenic worms (*P_{vha-6}::CUA-1.1::GFP::unc-54 3' UTR*) and (*P_{vha-6}::CUA-1.1::GFP::unc-54 3' UTR;cua-1(ok904)*) were grown for 2–2.5 days on NGM plates and analyzed using a COPAS Biosort. Error bars indicate mean \pm S.E. of ~200 worms (*, $p < 0.05$; **, $p < 0.01$; and ***, $p < 0.001$) (two-way ANOVA, Tukey's post hoc test). *E*, synchronized L1 stage wild-type N2 worms and transgenic worms (*P_{vha-6}::CUA-1.1::GFP::unc-54 3' UTR;cua-1(ok904)*) were fed control or *cua-1* RNAi bacteria and analyzed using a COPAS Biosort. TOF equivalent to zero indicates lethal phenotype. Error bars represent mean \pm S.E. of ~200 worms (***, $p < 0.001$) (two-way ANOVA, Tukey's post hoc test). *F*, total copper levels of L4/young adult stage wild-type worms grown on NGM plates with 0 or 50 μM supplemental copper as determined by ICP-MS. Error bars indicate mean \pm S.E. of six independent experiments. Means that do not share letters are significantly different from each other at $p = 0.05$ (two-way ANOVA, Tukey's post hoc test).

that intestinal CUA-1 is crucial for copper delivery to extra-intestinal tissues, depletion of *cua-1* by RNAi in both wild-type and *P_{vha-6}::CUA-1.1::GFP;cua-1(ok904)* worms resulted in improved growth under toxic copper conditions and growth inhibition under copper restriction as compared with vector RNAi (Fig. 4, C–E). To further understand the role of *cua-1* in copper metabolism, we measured total worm copper content

using ICP-MS. In the presence of 50 μM copper, either *cua-1* or *cuc-1* RNAi knockdown in wild-type worms resulted in ~30% lower total copper content than in control worms, whereas worms without copper supplementation exhibited similar total copper contents under both RNAi conditions (Fig. 4F). These results suggest that accumulation of copper under high dietary copper conditions is dependent on *cua-1*.

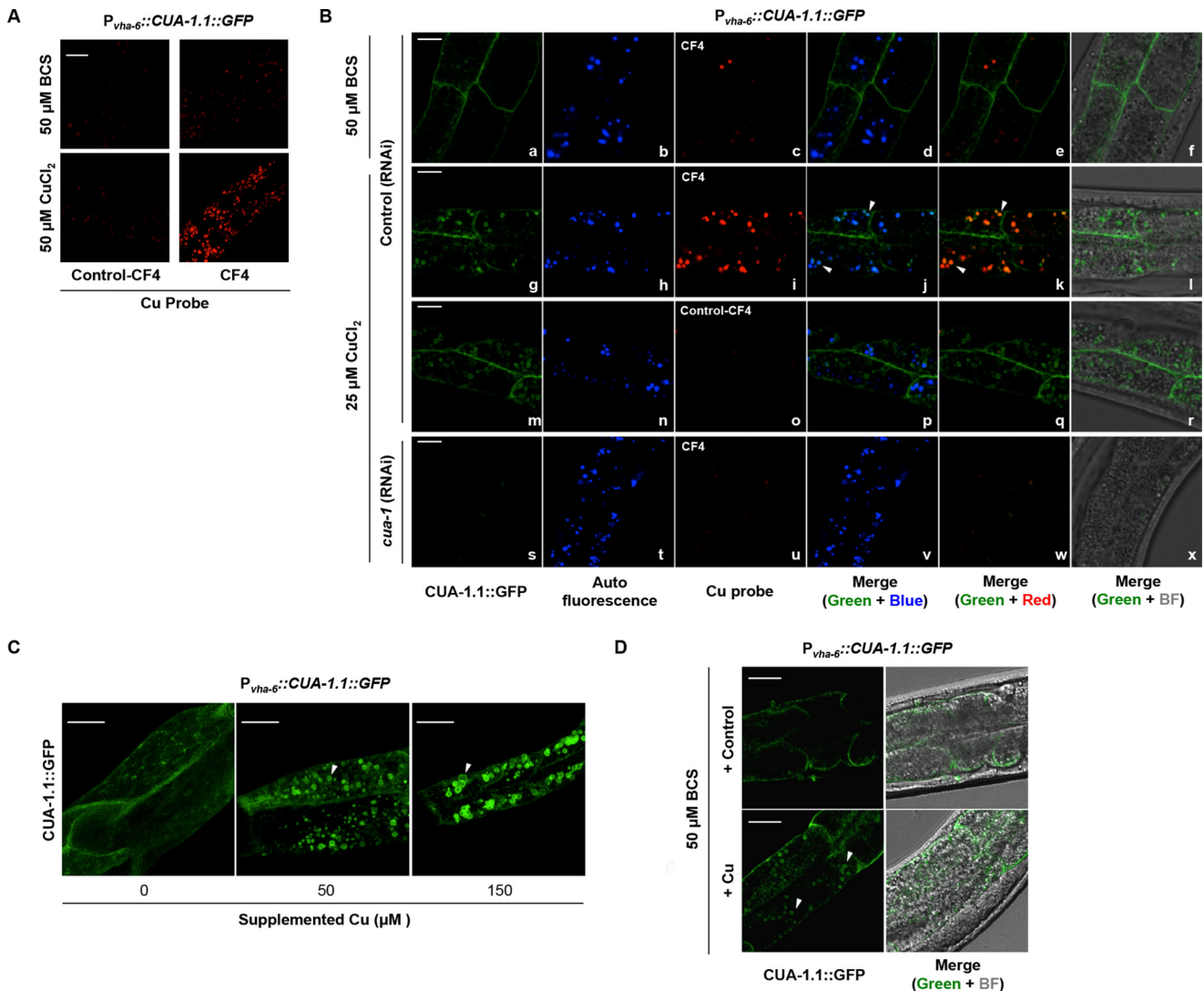


FIGURE 5. Localization of intestinal CUA-1.1 is altered by copper levels. *A*, fluorescence images of control-CF4 or CF4 copper probe staining in transgenic animals ($P_{vha-6}::CUA-1.1::GFP::unc-54$ 3' UTR) cultured with 50 μ M supplemental copper or BCS on NGM agar. *Scale bar*, 10 μ m. *B*, confocal images of transgenic animals ($P_{vha-6}::CUA-1.1::GFP::unc-54$ 3' UTR) expressing CUA-1.1::GFP in the intestine cultured with the copper probe CF4 or the control CF4 probe, the indicated levels of supplemental copper or BCS, and control or *cua-1* RNAi. Images show intestinal cells, and *arrowheads* indicate representative gut granules and copper probe positive vesicles overlapping with CUA-1.1::GFP. *Scale bar*, 10 μ m. *C*, confocal images were taken of transgenic animals ($P_{vha-6}::CUA-1.1::GFP::unc-54$ 3' UTR) under varying copper conditions. *Arrowheads* indicate representative CUA-1.1::GFP puncta. *Scale bar*, 10 μ m. *D*, transgenic animals ($P_{vha-6}::CUA-1.1::GFP::unc-54$ 3' UTR) were injected with M9 buffer containing either histidine alone or histidine with $CuCl_2$. *Arrowheads* indicate punctate of CUA-1.1::GFP. *Scale bar*, 20 μ m.

Intestinal CUA-1.1 Distribution Is Regulated by Copper Levels—Copper-responsive fluorescent probes have been used to visualize the distribution of labile copper in a variety of model systems (30–33). After conducting several pilot studies with a number of different copper probes in *C. elegans*, we selected the copper(I) probe CF4 based on its high specificity (see under “Experimental Procedures” for details). To investigate the dynamics of copper levels in the intestine, we pre-exposed worms expressing CUA-1.1::GFP in the intestine to either 50 μ M $CuCl_2$ or 50 μ M BCS followed by incubation with CF4. We observed that worms exposed to supplemental copper accumulated more fluorescence puncta in the intestine than worms treated with BCS, although a control CF4 probe, which lacks the copper-binding atoms but retains the same lipophilic dye platform, displayed weaker staining (Fig. 5A). These results

indicate that CF4 detects labile copper levels in vesicles of the intestine in *C. elegans*.

To test whether dietary copper alters CUA-1.1 localization, transgenic animals harboring a *cua-1.1* translational reporter driven by the *vha-6* promoter were grown under varying copper concentrations and then imaged using confocal microscopy. In the presence of 50 μ M BCS (Fig. 5B; supplemental Fig. S4) or no supplemental copper (data not shown), intestinal CUA-1.1::GFP localized predominantly to basolateral membranes (Fig. 5B, panels *a* and *f*), as well as low levels being detectable in intracellular compartments. We identified these compartments as Golgi, as some of them overlapped with the Golgi marker MANS::mCherry (supplemental Fig. S4). Strikingly, in the presence of 25 μ M supplemental copper, CUA-1.1::GFP was redistributed to a cellular compartment that was distinct from

CUA-1 Trafficking for Organismal Copper Balance

the Golgi (Fig. 5B, panels g and l; supplemental Fig. S4). CUA-1.1::GFP-containing vesicles overlapped with the autofluorescence of gut granules (Fig. 5B, panel j), an intestine-specific lysosome-related organelle, indicating that copper may be concentrated at these sites (34, 35).

To examine the relationship between CUA-1.1 and copper, transgenic animals expressing CUA-1.1::GFP were cultured with the copper probe CF4. In worms cultured with 25 μM copper, CF4 and CUA-1.1::GFP fluorescence overlapped almost completely, suggesting that CUA-1.1 localizes to the gut granules that concentrate copper in response to toxic levels of environmental copper (Fig. 5B, panel k). Additionally, intestinal CUA-1.1::GFP localization shifted from punctate staining to larger vesicles as worms were exposed to increasing concentrations of dietary copper (Fig. 5C). CUA-1.1::GFP expression in the intestine driven by the endogenous *cua-1* promoter rather than the *vha-6* promoter also showed similar trafficking in response to changes in dietary copper (supplemental Fig. S5A). Worms in which *cua-1* had been depleted by RNAi showed dramatically decreased levels of CF4 fluorescence in the intestine as compared with control worms (Fig. 5B, panels i and u) suggesting that CUA-1.1 acts to export copper to gut granules. In summary, CUA-1.1 mainly resides on the basolateral membranes under basal and copper-deficient conditions, but it localizes to gut granules in response to increasing dietary copper. Note that these changes are not due to copper-responsive elevation in protein abundance of intestinal CUA-1.1 ($P_{vha-6}::CUA-1.1::GFP$) in transgenic worms, as immunoblotting and COPAS Biosort analysis showed no significant differences in GFP levels when these worms were grown at varying copper levels (supplemental Fig. S6, A and B).

We next expressed CUA-1.1::GFP in the specialized epithelial cells of the *C. elegans* hypodermis using the hypodermis-specific *dpy-7* promoter (34). Confocal microscopy studies in transgenic worms expressing $P_{dpy-7}::CUA-1.1::GFP$ showed that in hypodermal tissues, plasma membrane localization of CUA-1.1::GFP was not affected by dietary copper, suggesting that copper-responsive trafficking of CUA-1.1 protein is intestine-specific (supplemental Fig. S5B).

To further explore whether the intracellular localization of intestinal CUA-1.1::GFP is altered by elevated copper status in the pseudocoelom, $\sim 100 \mu\text{g}$ of CuCl_2 per g of worm (wet weight) in M9 buffer was injected into the pseudocoelom of adult worms harboring the CUA-1.1::GFP transgene, which had been preincubated with 50 μM BCS. Interestingly, we observed a punctate pattern of CUA-1.1::GFP in the intestine of animals injected with copper, whereas M9-injected controls showed predominantly basolateral membrane localization (Fig. 5D), implying the existence of a systemic copper homeostasis mediated by the trafficking of intestinal CUA-1.1.

CUA-1.1 Is Required for Copper Detoxification in Intestine—To further investigate the dynamics of CUA-1.1 localization in response to sub-toxic doses of copper supplementation, we assayed CUA-1.1 colocalization with LysoTracker, a lysosome-specific fluorescent dye (35, 36). In the presence of 50 μM copper, LysoTracker was observed in intestinal vesicles surrounded by membrane-bound CUA-1.1::GFP (Fig. 6A). Upon RNAi knockdown of *cua-1*, the number and morphology of

LysoTracker-positive compartments did not change. However, RNAi knockdown *pgp-2*, which encodes an ABC transporter that is required for gut granule biogenesis and localizes to the gut granule membrane (35, 37), significantly reduced LysoTracker staining and prevented CUA-1.1::GFP-containing vesicle formation, whereas CUA-1.1::GFP was detected on the basolateral membrane (Fig. 6A). These results further suggest that CUA-1.1 localizes to the membranes of gut granules, and gut granules are the destination of copper sequestered by CUA-1.1 in the intestine when animals are exposed to high dietary copper.

To determine whether copper sequestration into gut granules by CUA-1.1 contributes to copper detoxification, we tested copper sensitivity by measuring the growth rate of *C. elegans* in the presence of increasing concentrations of copper. When compared with control worms, *pgp-2* depleted worms showed increased sensitivity to high copper, as they displayed a dose-dependent decrease in growth rate in response to copper (Fig. 6B). To quantify copper sequestration defects in gut granule-deficient worms, we measured total copper content in worms by ICP-MS. *pgp-2* mutant worms cultured in 50 μM copper displayed reduced total copper content as compared with wild-type worms (Fig. 6C). Consistent with previous reports, *pgp-2* mutant worms displayed lower zinc content independent of copper supplementation (supplemental Fig. S7, A and B) (8). These results indicate that copper deposition accounts for a significant proportion of total body copper in *C. elegans* and that gut granules are at least partially required for copper detoxification.

CUA-1 Isoforms Function Coordinately to Maintain Systemic Copper Levels—RNAseq assays with synchronized populations of worms treated with different copper or BCS levels revealed the existence of *cua-1.2* variant as annotated (Fig. 2A), although relative levels of the two isoforms have not been established.³ To examine whether intestinal CUA-1.2 also retains the capacity to traffic in response to a high copper diet, we generated transgenic worms expressing a CUA-1.2::GFP translational fusion driven from the intestinal *vha-6* promoter. Confocal microscopy analysis showed that CUA-1.2::GFP is localized to the basolateral membranes irrespective of dietary copper concentration (Fig. 7A). Additionally, CUA-1.2::GFP did not colocalize with autofluorescent gut granules under high copper conditions suggesting CUA-1.2 functions constantly at basolateral membranes. Because CUA-1.1 has an additional 122 amino acid sequences at the N terminus end compared with CUA-1.2, it is plausible that copper-dependent trafficking of CUA-1.1 to gut granules is dependent on trafficking motifs within this N-terminal segment.

Discussion

Dietary copper availability can fluctuate widely depending upon an organism's immediate environment, as would be the case in *C. elegans*, which lives in soil. In this study, we show that CUA-1.1 is expressed in intestinal cells and normally localizes to the basolateral membrane and intracellular compartments, such as the Golgi. When worms are exposed to higher copper

³ B.-E. Kim, unpublished data.

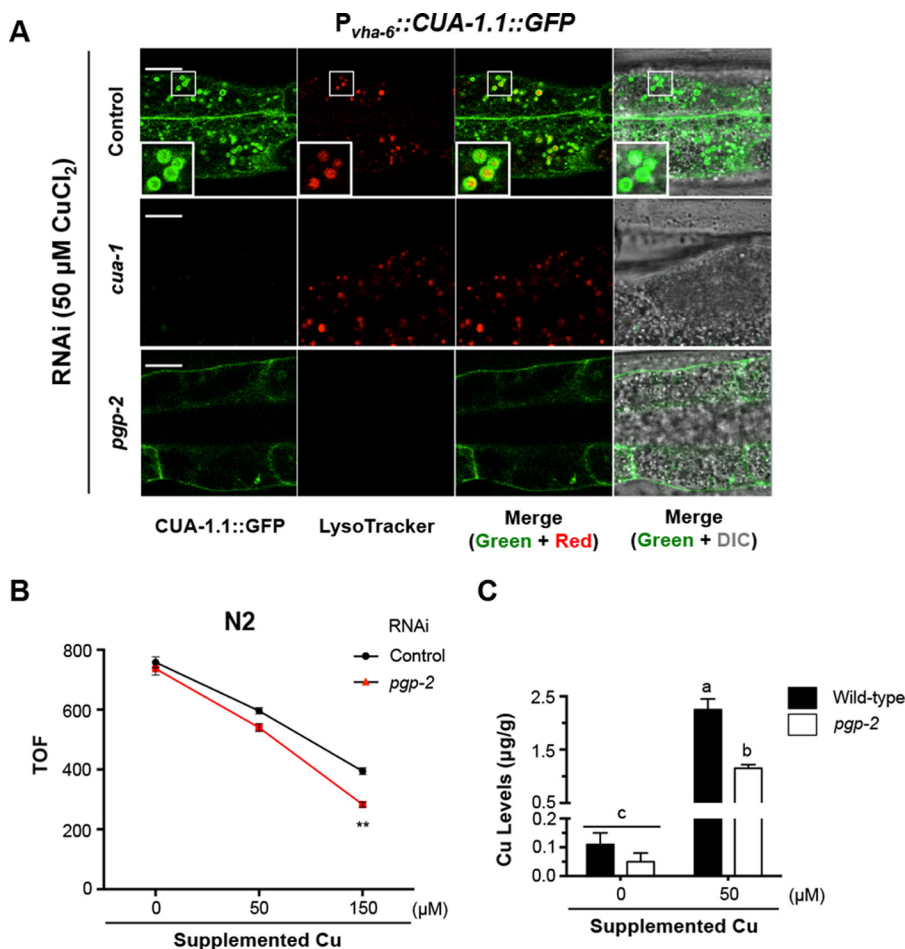


FIGURE 6. **CUA-1.1 sequesters excess copper to gut granules.** *A*, confocal images of transgenic animals ($P_{vha-6}::CUA-1.1::GFP::unc-54$ 3' UTR) exposed to varying RNAi conditions in the presence of 50 μM supplemental copper, followed by incubation with LysoTracker. *Boxed images in the top row are enlarged at the corner of each panel. Scale bar, 10 μm .* *B*, synchronized wild-type L1 larvae were cultured on RNAi plates supplemented with the indicated concentrations of copper for 2.5 days. TOF was determined using a COPAS Biosort. *Error bars indicate average \pm S.E. of two independent experiments. (**, $p < 0.01$, two-way ANOVA, Tukey's post hoc test.)* *C*, total copper levels of wild-type and *pgp-2(kx48)* worms as measured by ICP-MS. *Error bars show mean \pm S.E. of three independent experiments. Values marked with different letters are significantly different at $p = 0.05$ (two-way ANOVA, Tukey's post hoc test).*

levels, redistribution of intestinal CUA-1.1 promotes copper sequestration into lysosome-related organelles called gut granules. Defects in gut granule biogenesis lead to decreased copper accumulation and increased susceptibility to toxic copper levels. Together, these results suggest that copper homeostasis is regulated by altering the localization of intestinal CUA-1.1 to either the basolateral membrane for delivery of copper to peripheral tissues or to the gut granule membrane to prevent copper toxicity (Fig. 7B).

In *C. elegans*, which lack a liver, the intestine has been thought to perform functions associated with both the intestine and the liver (38). Worms encode only one copper exporter gene, *cua-1*, raising the question as to whether CUA-1 accomplishes some or all of the similar functions as ATP7A/B in the intestine and liver of mammals (20). We found that CUA-1 protein abundance in the intestine was not changed by dietary copper. Instead, both CUA-1 isoforms localize to basolateral membranes and intracellular compartments, including the Golgi under basal and copper-limiting conditions. The CUA-1.1 isoform alone redistributes to the gut granules when worms are exposed to high levels of copper, indicating that CUA-1 shares physiological features of mammalian ATP7A and

ATP7B. Enrichment of CUA-1.1 to the membrane of gut granules rather than the basolateral membrane of the intestine suggests a distinct role for intestinal CUA-1.1 in detoxification of excess copper in *C. elegans*. Although relocation of CUA-1.1 and ATP7B to the gut granules and apical membrane, respectively, in polarized cells is not identical, the direction of trafficking toward preventing systemic copper toxicity is similar. Taken together, these data indicate that intestinal CUA-1 functions as copper exporters in worms like ATP7A/B in both the intestine and liver of mammals to maintain copper balance in the body.

Given that CUA-1.2 lacks a portion of the N-terminal intracellular domain of CUA-1.1 and is targeted constitutively to the basolateral membrane even under copper-loaded conditions, necessary trafficking information may exist in the first 122 amino acids of CUA-1.1 for copper responsiveness and correct targeting to gut granules. Several intriguing questions arise from this observation. What route does CUA-1.1 take to reach gut granules when intracellular copper is increased? Where within the first 122 amino acids is the crucial targeting signal? What cellular machinery recognizes the copper signal? One possible sorting complex is the biogenesis of lysosome-related

CUA-1 Trafficking for Organismal Copper Balance

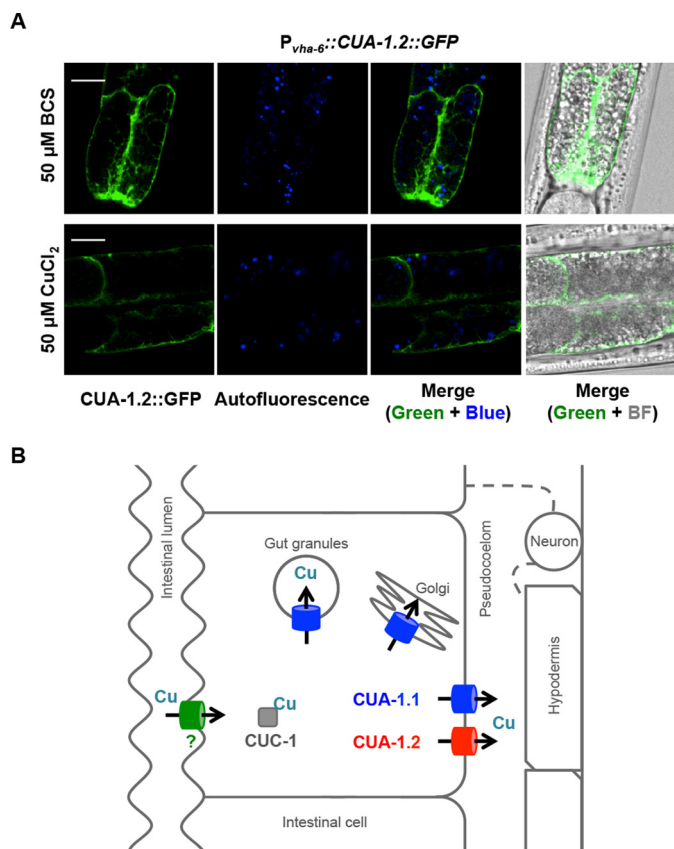


FIGURE 7. Copper homeostasis in worms is maintained by distinctly localized intestinal CUA-1 isoforms. *A*, confocal images of transgenic animals ($P_{vha-6}::CUA-1.2::GFP::unc-54$ 3' UTR) expressing CUA-1.2::GFP in the intestine in the presence of 50 μ M supplemental copper or BCS. Scale bar, 10 μ m. *B*, model of copper homeostasis in *C. elegans* is shown. Dietary copper ions are transported from the lumen of the intestine to the enterocytes by an unidentified copper importer, and CUC-1 delivers copper to CUA-1. Under basal copper or copper-deficient conditions, CUA-1.1 isoform localizes to the basolateral membrane and Golgi to either export copper ions to peripheral tissues or to direct copper into the secretory pathway. CUA-1.2 consistently localizes to the basolateral membrane of enterocytes regardless of copper conditions. CUA-1.1 is redistributed to the gut-granule membranes in response to elevated copper levels to promote copper detoxification in *C. elegans*.

organelles complex-1 (BLOC-1), which is a known regulator of intracellular trafficking to lysosome-related organelles in mammals, *Drosophila*, and *C. elegans* (39–41). ATP7A is known to supply copper to melanosomes in a BLOC-1-dependent manner in mammalian cells, and BLOC-1 subunits are also required for the proper trafficking of gut granule cargo in worms (39, 42). Given that CUA-1.1 localizes to gut granules and that ATP7A localizes to melanosomes in response to elevated levels of copper, redistribution of the copper exporter may require the BLOC-1 complex and related sorting proteins in metazoans.

We have determined that gut granules function to sequester excess copper via CUA-1.1 in the intestine. Ablation of *cua-1* by RNAi does not interfere with the formation of gut granules, but copper was not readily detected by a copper probe in gut granules upon the loss of CUA-1.1. RNAi depletion of *pgp-2* genes resulted in significantly reduced numbers of gut granules and increased sensitivity to copper toxicity. However, whether stored copper is capable of being reutilized under copper-limiting conditions was not determined. Studies by Kornfeld and co-workers (8) have shown that gut granules act to detoxify and

store dietary zinc via the CDF-2 zinc exporter. When worms were exposed to high concentrations of dietary zinc, gut granules displayed a bilobed morphology, which was not observed in our studies with CUA-1.1 and high dietary copper. We speculate that gut granules may function as a central site of metal storage to prevent its cytotoxicity. This is specifically relevant because depletion of the metallothionein genes *mtl-1* and *mtl-2* by RNAi does not result in the expected enhanced susceptibility to copper toxicity (43, 44), raising the possibility that *C. elegans* may adopt a protective mechanism to withstand an environmental challenge of toxic copper by sequestering copper to an intracellular location via CUA-1.1.

Unexpectedly, we observed that CUA-1.1 expression is up-regulated in response to dietary copper deficiency in the hypodermis when expressed under the control of an endogenous promoter. Given that CUA-1.1 abundance was not altered under the *dpy-7* promoter, and that *cua-1* transcript levels increased under copper-limiting conditions, hypodermal *cua-1* may respond to copper deficiency transcriptionally. MTF-1 is known to transcriptionally induce both ATP7 and metallothionein expression in *Drosophila*, but no MTF-1 homolog has been defined in *C. elegans* (45–48). MTF-1-independent metal-responsive transcription factors have been identified, suggesting the existence of other copper-responsive transcription factors that could regulate *cua-1* expression in the hypodermis (43, 49). CUA-1 in the hypodermis may deliver copper to the secretory pathway for copper incorporation into copper-dependent enzymes. Another possibility is that the hypodermis acts as a copper storage compartment that can release copper to peripheral tissues by increasing CUA-1.1 expression when worms are in a copper-deficient environment. When CUA-1.1 is highly expressed in the hypodermis under dietary copper restriction, most CUA-1.1 localizes to plasma membranes. Notably, the hypodermis is known to act as a major fat storage site in worms by accumulation of lipid droplets (50, 51).

Organs communicate to ensure that intestinally derived micronutrients are distributed appropriately throughout tissues in the body, balancing cellular requirements against toxicity (52, 53). We injected copper into the pseudocoelom of adult worms expressing CUA-1.1::GFP that had been precultured with BCS. Interestingly, worms injected with copper showed a punctate distribution of CUA-1.1::GFP, implying that CUA-1.1 responds to copper status in the pseudocoelom and/or copper overload in peripheral tissues. In mammals, iron overload results in the liver producing elevated levels of secreted hepcidin that interacts with the ferroportin iron exporter on the basolateral membrane of intestinal epithelial cells as well as on macrophages. Hepcidin causes ferroportin to be internalized, resulting in decreased iron entry into the bloodstream (53, 54). In *C. elegans*, several neuropeptides are known to mediate intestinal function to regulate metabolism and development (55–57), although a hepcidin homolog has not been found. Cardiac copper deficiency caused by depletion of the *Ctrl* copper importer in the heart induced a significant up-regulation of ATP7A in the intestine of mice, which may lead to increased copper supply into circulation (58). This study suggested that cross-talk may take place between tissue types to coordinate systemic copper homeostasis. In *C. elegans*, although entero-

cyte-autonomous copper homeostasis regulation may result in a sufficient organismal copper balance in general, another possibility is that intestinal CUA-1.1 is regulated via an inter-organ communication network. A cellular component responsible for copper-dependent CUA-1.1 trafficking in the intestine may be the molecular link by which the enterocytes sense and respond to extraintestinal copper status. Future studies to characterize how intestinal copper acquisition and distribution are regulated at the systemic level may lead to the discovery of new pathways of organismal copper trafficking.

Experimental Procedures

Worm Culture and Strains—*C. elegans* were cultivated at 20 °C on NGM plates seeded with *E. coli* OP50 or HT115(DE3) as a food source. Strain information (including the Bristol N2 strain, transgenic strains, and deletion strains used in this study) is detailed in [supplemental Table S1](#). Several worm strains were obtained from the *Caenorhabditis* Genetics Center, which is funded by the National Institutes of Health Office of Research Infrastructure Programs. The presence of the *cua-1* (*ok904*) allele was confirmed by sequencing of the *cua-1* locus using the following primers: 5'-CCAGCTAACCACAATTGT-TTTCG-3' and 5'-CGAATCCTTCTCGTCGTCATTTTC-3'. Genotypes of transgenic animals and mutant worms were confirmed by DNA sequencing or PCR. CuCl₂ was used as the source for copper supplementation in NGM dishes and media in all experiments.

Worm Analysis Using COPAS Biosort or Microscopy—Gravid hermaphrodites were bleached to release their eggs, which were allowed to hatch and arrest at the L1 stage in M9 buffer overnight. The resultant age-synchronized L1 larvae were cultured on NGM plates for ~2.5 days. Worms from each condition (~200 worms) were analyzed for time of flight (length), extinction (width), and GFP fluorescence using a COPAS Biosort FP-250 (Union Biometrica). To visualize live worms, animals were paralyzed in M9 buffer containing 10 mM sodium azide (NaN₃) and mounted on agarose pads. GFP, mCherry, copper probe CF4, autofluorescence, and LysoTracker fluorescence in worms were imaged using an SP5 X confocal microscope (Leica).

ICP-MS—Metal contents of worms and MEFs were measured using ICP-MS as described previously (59). Values were normalized to wet weight of worms or cells. For sample preparation, synchronized L1 worms were grown on 10-cm NGM plates seeded with OP50 or HT115 RNAi bacteria and supplemented with the indicated amounts of copper or BCS. Worm or cell pellets were collected and washed extensively with M9 buffer or PBS, respectively, transferred to acid-washed tubes, and frozen at -80 °C. At least three independent biological replicates were analyzed.

qRT-PCR—Synchronized larvae were grown to the L4/young adult stage on NGM plates seeded with OP50 bacteria and supplemented with indicated concentrations of copper or BCS. Then the worms were extensively washed with M9 buffer and collected for RNA isolation. Briefly, worms were resuspended in TRIzol (Invitrogen) reagent followed by lysis using a FastPrep-24 (MP Biomedicals) homogenizer in Lysing Matrix Tubes (MP Biomedicals). Total RNA was isolated using TRIzol

and treated with DNase I (Ambion), and cDNA was produced using SuperScript VILO Master Mix (Invitrogen). Real time PCR was performed on an Agilent Mx3005P qPCR system thermocycler (Agilent Genomics) using SYBR Green JumpStart Taq ReadyMix (Sigma). Expression levels of *cua-1* were compared with an internal GAPDH (*gpd-2*) control, and the fold changes were determined using the $2^{-\Delta\Delta C_t}$ method (60). The primers used for qPCR were as follows: *cua-1*, 5'-TGGCACA-ATCACCGAAGGAC-3' and 5'-CAATCGGATGCTCCGAC-AAA-3'; and *gpd-2*, 5'-TGCTCACGAGGGAGACTAC-3' and 5'-CGCTGGACTCAACGCATAG-3'.

Plasmid Construction and Transgenic Strain Generation—To generate *C. elegans* expression plasmids, gene-specific gateway *attB* primers were used to amplify DNA sequences such as promoters, ORFs, and 3'-UTRs. Purified DNA fragments were recombined into donor vectors first and then into expression plasmids using Gateway recombination reactions (Invitrogen). For mammalian cell expression plasmids, the GFP-tagged ORF of CUA-1 was digested with NheI and BamHI and ligated into the pEGFP-C1 vector (Clontech). Transgenic animals were produced by introducing transcriptional or translational reporters into *unc-119* worms using the PDS-1000 particle delivery system (Bio-Rad) for bombardment transformation (13, 15).

RNA Interference (RNAi)—RNAi bacteria strains against *cua-1* (Y76A2A.2) and *pgp-2* (C34G6.4) were obtained from the Ahringer feeding library (61), and *cuc-1* (ZK652.11) was obtained from the ORFeome-based RNAi library (62). Bacteria transformed with the empty L4440 vector were used as a negative RNAi control. Synchronized L1 animals were grown on RNAi plates (NGM dishes containing 2 mM isopropyl 1-thio- β -D-galactopyranoside, 12 μ g/ml tetracycline, and 50 μ g/ml carbenicillin) that were seeded with HT115(DE3) bacteria expressing dsRNA for each gene.

Cell Culture and Immunoblotting—*Atp7a*^{+/+} and *Atp7a*^{-/-} MEFs were cultured in Dulbecco's modified Eagle's medium (DMEM; Lonza) supplemented with 10% (v/v) heat-inactivated fetal bovine serum (FBS; Atlanta Biologicals) and 100 units/ml penicillin/streptomycin (Lonza). The plasmid expressing CUA-1.1::GFP was transfected to *Atp7a*^{-/-} MEFs using PolyJet (SigmaGen Laboratories). All cells were cultured under 5% CO₂ at 37 °C. Cells at ~70% confluence were collected and washed three times with ice-cold PBS, pH 7.4. Cell pellets were suspended in about five times their volume in ice-cold cell lysis buffer (PBS, pH 7.4, 1% Triton X-100, 0.1% SDS, 1 mM EDTA) containing Halt protease inhibitor mixture (Thermo Scientific), briefly vortexed, and incubated for 1 h. Early stage adult worms grown from synchronized larvae were collected and washed with M9 buffer. Worms were resuspended in the same lysis buffer followed by disruption using a FastPrep-24 (MP Biomedicals) homogenizer in the presence of glass beads. The same lysis buffer was used for disruption of MEFs on ice for 30 min. Cell suspensions and worm lysates were centrifuged at 16,000 \times g at 4 °C for 15 min. After centrifugation, the clarified lysates were used for immunoblotting, and protein concentrations were measured using the BCA protein assay kit (Thermo Scientific). Samples (100 μ g/lane) were fractionated on a 4–20% gradient gel (Bio-Rad). The anti-ATP7A antibody (a gift

CUA-1 Trafficking for Organismal Copper Balance

from Dr. Stephen G. Kaler, National Institutes of Health, Bethesda), anti-GFP (Covance), and anti-tubulin antibody (Sigma) were used at a 1:1000 dilution. The anti-CCS antibody (Santa Cruz Biotechnology) and anti-GAPDH antibody (Sigma) were used at 1:4000 dilution and 1:10,000 dilution, respectively. Horseradish peroxidase-conjugated anti-rabbit or anti-mouse IgG (Rockland Immunochemicals) was used as the secondary antibody for immunoblotting (1:5000 dilution). Immunoblots were detected using SuperSignal West Pico Chemiluminescent Substrate reagents (Thermo Fisher Scientific) using a chemidocumentation imaging system (Bio-Rad).

Staining with the Copper Probe CF4 and LysoTracker—The Copper Fluor-4 (CF4) sensor combines a piperidine-substituted rhodol with a trifluoromethyl-substituted bottom ring bearing a thioether receptor, along with a matched control Copper Fluor-4 (Control CF4) dye that lacks the copper-responsive receptor to help distinguish between copper-dependent and dye-dependent responses (30, 63). Replacement of the thioether-rich receptor arms for copper recognition in CF4 by isostructural octyl groups in control CF4 provides a mimic of the size, shape, and hydrophobicity of thioethers but do not bind copper, offering a matched pair of probes to disentangle copper-dependent fluorescence responses from potential dye-dependent ones. We used the Rhodol-based CF4 probe and control CF4 probe (both final concentrations of 25 μM) for staining copper(I) in intact worms and 2 μM LysoTracker Red DND-99 (Invitrogen) for detecting gut granules. Both chemicals were prepared in M9 buffer and dispensed onto NGM plates (8). L3 stage worms were cultured on these dishes for 12–16 h in the dark. Postincubation, the stained worms were transferred to seeded NGM plates containing copper concentrations equivalent to treatment conditions. After 2 h of incubation, worms were collected and washed three times with M9 buffer and imaged via confocal microscopy.

Copper Microinjection Experiments—To deliver copper directly to the basolateral side of the intestine and peripheral tissues, CuCl_2 solution was microinjected into the pseudocoelom in the posterior region of young adult worms that had been grown in 50 μM BCS-treated NGM dishes. Histidine or CuCl_2 with histidine (1:2 molar ratio) diluted in M9 buffer was injected to worms using an Eppendorf Femtojet microinjector attached to a Leica inverted microscope under specified settings (injection pressure = 30 p.s.i., compensation pressure = 4.5 p.s.i., injection time = 4 s). Worms were recovered on seeded plates for 6 h and then mounted on 2% agarose pads for imaging.

Bioinformatics and Statistics—Clustal Omega and ClustalW2 were used to generate a multiple sequence alignment and phylogenetic tree of a subset of *cua-1* homologs (64). Transmembrane helices and copper-binding motifs of CUA-1 homologs were predicted using Trans-Membrane prediction using Hidden Markov Models and the Conserved Domain Database (22). Statistical significance was determined using a one-way or two-way ANOVA followed by Tukey's post hoc test in GraphPad Prism, Version 6 (GraphPad Software). All data are presented as mean \pm S.E., and *p* values less than 0.05 were considered to be statistically significant.

Author Contributions—H. C. and B.-E. K. conceived the study. H. C. conducted most of the experiments, analyzed the data, and wrote most of the paper with B.-E. K. A. K. S. conducted live worm imaging with the CF4 copper probe and copper microinjection experiments. J. L. conducted ICP-MS analysis. J. C. and S. J. generated the CF4 and control-CF4 probes. All authors reviewed the results and approved the final version of the manuscript.

Acknowledgments—We thank members of the Kim laboratory for helpful suggestions, technical assistance, and critical reading of this manuscript. We thank members of Dr. Iqbal Hamza's laboratory (University of Maryland, College Park) for technical assistance and expertise in *C. elegans* genetics and cell biology as well as for discussions regarding the work, and Dr. Tamara Korolnek for critical reading of this manuscript. We thank Dr. Stephen G. Kaler (National Institutes of Health, Bethesda) for the anti-ATP7A antibody, and Dr. Michael J. Petris (University of Missouri, Columbia) for ATP7A knock-out MEFs. We thank Dr. Christopher J. Chang (University of California, Berkeley) for discussion and help in providing and using the CF4 and Control-CF4 probes. The worm strain expressing MANS::mCherry was generously provided by Dr. Christopher Rongo (Rutgers The State University of New Jersey). The COPAS Biosort instrument was purchased from funds supported by a supplement to National Institutes of Health Grant DK074797 (to I. H.).

References

1. Kim, B. E., Nevitt, T., and Thiele, D. J. (2008) Mechanisms for copper acquisition, distribution and regulation. *Nat. Chem. Biol.* **4**, 176–185
2. Nevitt, T., Ohrvik, H., and Thiele, D. J. (2012) Charting the travels of copper in eukaryotes from yeast to mammals. *Biochim. Biophys. Acta* **1823**, 1580–1593
3. Madsen, E., and Gitlin, J. D. (2007) Copper and iron disorders of the brain. *Annu. Rev. Neurosci.* **30**, 317–337
4. La Fontaine, S., and Mercer, J. F. (2007) Trafficking of the copper-ATPases, ATP7A and ATP7B: role in copper homeostasis. *Arch. Biochem. Biophys.* **463**, 149–167
5. Nyasae, L., Bustos, R., Braiterman, L., Eipper, B., and Hubbard, A. (2007) Dynamics of endogenous ATP7A (Menkes protein) in intestinal epithelial cells: copper-dependent redistribution between two intracellular sites. *Am. J. Physiol. Gastrointest. Liver Physiol.* **292**, G1181–G1194
6. Monty, J. F., Llanos, R. M., Mercer, J. F., and Kramer, D. R. (2005) Copper exposure induces trafficking of the Menkes protein in intestinal epithelium of ATP7A transgenic mice. *J. Nutr.* **135**, 2762–2766
7. Anderson, C. P., and Leibold, E. A. (2014) Mechanisms of iron metabolism in *Caenorhabditis elegans*. *Front. Pharmacol.* **5**, 113
8. Roh, H. C., Collier, S., Guthrie, J., Robertson, J. D., and Kornfeld, K. (2012) Lysosome-related organelles in intestinal cells are a zinc storage site in *C. elegans*. *Cell Metab.* **15**, 88–99
9. Severance, S., and Hamza, I. (2009) Trafficking of heme and porphyrins in metazoa. *Chem. Rev.* **109**, 4596–4616
10. Maduro, M. F., and Rothman, J. H. (2002) Making worm guts: the gene regulatory network of the *Caenorhabditis elegans* endoderm. *Dev. Biol.* **246**, 68–85
11. Simon, T. C., and Gordon, J. I. (1995) Intestinal epithelial cell differentiation: new insights from mice, flies and nematodes. *Curr. Opin. Genet. Dev.* **5**, 577–586
12. Meredith, D., and Boyd, C. A. (2000) Structure and function of eukaryotic peptide transporters. *Cell. Mol. Life Sci.* **57**, 754–778
13. Korolnek, T., Zhang, J., Beardsley, S., Scheffer, G. L., and Hamza, I. (2014) Control of metazoan heme homeostasis by a conserved multidrug resistance protein. *Cell Metab.* **19**, 1008–1019
14. Romney, S. J., Newman, B. S., Thacker, C., and Leibold, E. A. (2011) HIF-1 regulates iron homeostasis in *Caenorhabditis elegans* by activation and

- inhibition of genes involved in iron uptake and storage. *PLoS Genet.* **7**, e1002394
15. Chen, C., Samuel, T. K., Sinclair, J., Dailey, H. A., and Hamza, I. (2011) An intercellular heme-trafficking protein delivers maternal heme to the embryo during development in *C. elegans*. *Cell* **145**, 720–731
 16. Davis, D. E., Roh, H. C., Deshmukh, K., Bruinsma, J. J., Schneider, D. L., Guthrie, J., Robertson, J. D., and Kornfeld, K. (2009) The cation diffusion facilitator gene *cdf-2* mediates zinc metabolism in *Caenorhabditis elegans*. *Genetics* **182**, 1015–1033
 17. Rao, A. U., Carta, L. K., Lesuisse, E., and Hamza, I. (2005) Lack of heme synthesis in a free-living eukaryote. *Proc. Natl. Acad. Sci. U.S.A.* **102**, 4270–4275
 18. Wakabayashi, T., Nakamura, N., Sambongi, Y., Wada, Y., Oka, T., and Futai, M. (1998) Identification of the copper chaperone, CUC-1, in *Caenorhabditis elegans*: tissue specific co-expression with the copper transporting ATPase, CUA-1. *FEBS Lett.* **440**, 141–146
 19. Southon, A., Burke, R., Norgate, M., Batterham, P., and Camakaris, J. (2004) Copper homeostasis in *Drosophila melanogaster* S2 cells. *Biochem. J.* **383**, 303–309
 20. Sambongi, Y., Wakabayashi, T., Yoshimizu, T., Omote, H., Oka, T., and Futai, M. (1997) *Caenorhabditis elegans* cDNA for a Menkes/Wilson disease gene homologue and its function in a yeast CCC2 gene deletion mutant. *J. Biochem.* **121**, 1169–1175
 21. C. elegans Deletion Mutant Consortium. (2012) Large-scale screening for targeted knockouts in the *Caenorhabditis elegans* genome. *G3* **2**, 1415–1425
 22. Krogh, A., Larsson, B., von Heijne, G., and Sonnhammer, E. L. (2001) Predicting transmembrane protein topology with a hidden Markov model: application to complete genomes. *J. Mol. Biol.* **305**, 567–580
 23. Edgley, M. L., Baillie, D. L., Riddle, D. L., and Rose, A. M. (2006) Genetic balancers. *WormBook* 2006, 1–32
 24. Wang, Y., Zhu, S., Weisman, G. A., Gitlin, J. D., and Petris, M. J. (2012) Conditional knockout of the Menkes disease copper transporter demonstrates its critical role in embryogenesis. *PLoS One* **7**, e43039
 25. Bertinato, J., and L'Abbé, M. R. (2003) Copper modulates the degradation of copper chaperone for Cu,Zn superoxide dismutase by the 26 S proteasome. *J. Biol. Chem.* **278**, 35071–35078
 26. Caruano-Yzermans, A. L., Bartnikas, T. B., and Gitlin, J. D. (2006) Mechanisms of the copper-dependent turnover of the copper chaperone for superoxide dismutase. *J. Biol. Chem.* **281**, 13581–13587
 27. Qadota, H., Inoue, M., Hikita, T., Köppen, M., Hardin, J. D., Amano, M., Moerman, D. G., and Kaibuchi, K. (2007) Establishment of a tissue-specific RNAi system in *C. elegans*. *Gene* **400**, 166–173
 28. Oka, T., Toyomura, T., Honjo, K., Wada, Y., and Futai, M. (2001) Four subunit isoforms of *Caenorhabditis elegans* vacuolar H⁺-ATPase. Cell-specific expression during development. *J. Biol. Chem.* **276**, 33079–33085
 29. Chen, B., Jiang, Y., Zeng, S., Yan, J., Li, X., Zhang, Y., Zou, W., and Wang, X. (2010) Endocytic sorting and recycling require membrane phosphatidylserine asymmetry maintained by TAT-1/CHAT-1. *PLoS Genet.* **6**, e1001235
 30. Dodani, S. C., Firl, A., Chan, J., Nam, C. I., Aron, A. T., Onak, C. S., Ramos-Torres, K. M., Paek, J., Webster, C. M., Feller, M. B., and Chang, C. J. (2014) Copper is an endogenous modulator of neural circuit spontaneous activity. *Proc. Natl. Acad. Sci. U.S.A.* **111**, 16280–16285
 31. Hong-Hermesdorf, A., Miethke, M., Gallaher, S. D., Kropat, J., Dodani, S. C., Chan, J., Barupala, D., Domaille, D. W., Shirasaki, D. I., Loo, J. A., Weber, P. K., Pett-Ridge, J., Stemmler, T. L., Chang, C. J., and Merchant, S. S. (2014) Subcellular metal imaging identifies dynamic sites of Cu accumulation in *Chlamydomonas*. *Nat. Chem. Biol.* **10**, 1034–1042
 32. Dodani, S. C., Leary, S. C., Cobine, P. A., Winge, D. R., and Chang, C. J. (2011) A targetable fluorescent sensor reveals that copper-deficient SCO1 and SCO2 patient cells prioritize mitochondrial copper homeostasis. *J. Am. Chem. Soc.* **133**, 8606–8616
 33. Aron, A. T., Ramos-Torres, K. M., Cotruvo, J. A., Jr., and Chang, C. J. (2015) Recognition- and reactivity-based fluorescent probes for studying transition metal signaling in living systems. *Acc. Chem. Res.* **48**, 2434–2442
 34. Gilleard, J. S., Barry, J. D., and Johnstone, I. L. (1997) cis regulatory requirements for hypodermal cell-specific expression of the *Caenorhabditis elegans* cuticle collagen gene *dpy-7*. *Mol. Cell. Biol.* **17**, 2301–2311
 35. Hermann, G. J., Schroeder, L. K., Hieb, C. A., Kershner, A. M., Rabbitts, B. M., Fonarev, P., Grant, B. D., and Priess, J. R. (2005) Genetic analysis of lysosomal trafficking in *Caenorhabditis elegans*. *Mol. Biol. Cell* **16**, 3273–3288
 36. Kostich, M., Fire, A., and Fambrough, D. M. (2000) Identification and molecular-genetic characterization of a LAMP/CD68-like protein from *Caenorhabditis elegans*. *J. Cell Sci.* **113**, 2595–2606
 37. Schroeder, L. K., Kremer, S., Kramer, M. J., Currie, E., Kwan, E., Watts, J. L., Lawrenson, A. L., and Hermann, G. J. (2007) Function of the *Caenorhabditis elegans* ABC transporter PGP-2 in the biogenesis of a lysosome-related fat storage organelle. *Mol. Biol. Cell* **18**, 995–1008
 38. McGhee, J. D. (2007) The *C. elegans* intestine. *WormBook* 2007, 1–36
 39. Hermann, G. J., Scavarda, E., Weis, A. M., Saxton, D. S., Thomas, L. L., Salesky, R., Somhegyi, H., Curtin, T. P., Barrett, A., Foster, O. K., Vine, A., Erlich, K., Kwan, E., Rabbitts, B. M., and Warren, K. (2012) *C. elegans* BLOC-1 functions in trafficking to lysosome-related gut granules. *PLoS one* **7**, e43043
 40. Cheli, V. T., Daniels, R. W., Godoy, R., Hoyle, D. J., Kandachar, V., Starcevic, M., Martinez-Agosto, J. A., Poole, S., DiAntonio, A., Lloyd, V. K., Chang, H. C., Krantz, D. E., and Dell'Angelica, E. C. (2010) Genetic modifiers of abnormal organelle biogenesis in a *Drosophila* model of BLOC-1 deficiency. *Hum. Mol. Genet.* **19**, 861–878
 41. Cheli, V. T., and Dell'Angelica, E. C. (2010) Early origin of genes encoding subunits of biogenesis of lysosome-related organelles complex-1, -2 and -3. *Traffic* **11**, 579–586
 42. Setty, S. R., Tenza, D., Sviderskaya, E. V., Bennett, D. C., Raposo, G., and Marks, M. S. (2008) Cell-specific ATP7A transport sustains copper-dependent tyrosinase activity in melanosomes. *Nature* **454**, 1142–1146
 43. Roh, H. C., Dimitrov, I., Deshmukh, K., Zhao, G., Warnhoff, K., Cabrera, D., Tsai, W., and Kornfeld, K. (2015) A modular system of DNA enhancer elements mediates tissue-specific activation of transcription by high dietary zinc in *C. elegans*. *Nucleic Acids Res.* **43**, 803–816
 44. Taubert, S., Hansen, M., Van Gilst, M. R., Cooper, S. B., and Yamamoto, K. R. (2008) The mediator subunit MDT-15 confers metabolic adaptation to ingested material. *PLoS Genet.* **4**, e1000021
 45. Radtke, F., Heuchel, R., Georgiev, O., Hergersberg, M., Gariglio, M., Dembic, Z., and Schaffner, W. (1993) Cloned transcription factor MTF-1 activates the mouse metallothionein I promoter. *EMBO J.* **12**, 1355–1362
 46. Brugnera, E., Georgiev, O., Radtke, F., Heuchel, R., Baker, E., Sutherland, G. R., and Schaffner, W. (1994) Cloning, chromosomal mapping and characterization of the human metal-regulatory transcription factor MTF-1. *Nucleic Acids Res.* **22**, 3167–3173
 47. Zhang, B., Egli, D., Georgiev, O., and Schaffner, W. (2001) The *Drosophila* homolog of mammalian zinc finger factor MTF-1 activates transcription in response to heavy metals. *Mol. Cell. Biol.* **21**, 4505–4514
 48. Bahadorani, S., Bahadorani, P., Marcon, E., Walker, D. W., and Hilliker, A. J. (2010) A *Drosophila* model of Menkes disease reveals a role for DmATP7 in copper absorption and neurodevelopment. *Dis. Model. Mech.* **3**, 84–91
 49. Rutherford, J. C., and Bird, A. J. (2004) Metal-responsive transcription factors that regulate iron, zinc, and copper homeostasis in eukaryotic cells. *Eukaryot. Cell* **3**, 1–13
 50. Mak, H. Y. (2012) Lipid droplets as fat storage organelles in *Caenorhabditis elegans*: thematic review series: lipid droplet synthesis and metabolism: from yeast to man. *J. Lipid Res.* **53**, 28–33
 51. Palgunow, D., Klapper, M., and Döring, F. (2012) Dietary restriction during development enlarges intestinal and hypodermal lipid droplets in *Caenorhabditis elegans*. *PLoS One* **7**, e46198
 52. Kautz, L., Jung, G., Valore, E. V., Rivella, S., Nemeth, E., and Ganz, T. (2014) Identification of erythroferrone as an erythroid regulator of iron metabolism. *Nat. Genet.* **46**, 678–684
 53. Nemeth, E., Tuttle, M. S., Powelson, J., Vaughn, M. B., Donovan, A., Ward, D. M., Ganz, T., and Kaplan, J. (2004) Hepcidin regulates cellular iron efflux by binding to ferroportin and inducing its internalization. *Science* **306**, 2090–2093

CUA-1 Trafficking for Organismal Copper Balance

54. Muckenthaler, M. U. (2008) Fine tuning of hepcidin expression by positive and negative regulators. *Cell Metab.* **8**, 1–3
55. Noble, T., Stieglitz, J., and Srinivasan, S. (2013) An integrated serotonin and octopamine neuronal circuit directs the release of an endocrine signal to control *C. elegans* body fat. *Cell Metab.* **18**, 672–684
56. Hung, W. L., Wang, Y., Chitturi, J., and Zhen, M. (2014) A *Caenorhabditis elegans* developmental decision requires insulin signaling-mediated neuron-intestine communication. *Development* **141**, 1767–1779
57. Chew, Y. L., Götz, J., and Nicholas, H. R. (2015) Neuronal protein with tau-like repeats (PTL-1) regulates intestinal SKN-1 nuclear accumulation in response to oxidative stress. *Aging Cell* **14**, 148–151
58. Kim, B. E., Turski, M. L., Nose, Y., Casad, M., Rockman, H. A., and Thiele, D. J. (2010) Cardiac copper deficiency activates a systemic signaling mechanism that communicates with the copper acquisition and storage organs. *Cell Metab.* **11**, 353–363
59. Nose, Y., Kim, B. E., and Thiele, D. J. (2006) Ctr1 drives intestinal copper absorption and is essential for growth, iron metabolism, and neonatal cardiac function. *Cell Metab.* **4**, 235–244
60. Livak, K. J., and Schmittgen, T. D. (2001) Analysis of relative gene expression data using real-time quantitative PCR and the $2(-\Delta\Delta C(T))$ method. *Methods* **25**, 402–408
61. Kamath, R. S., Fraser, A. G., Dong, Y., Poulin, G., Durbin, R., Gotta, M., Kanapin, A., Le Bot, N., Moreno, S., Sohrmann, M., Welchman, D. P., Zipperlen, P., and Ahringer, J. (2003) Systematic functional analysis of the *Caenorhabditis elegans* genome using RNAi. *Nature* **421**, 231–237
62. Rual, J. F., Ceron, J., Koreth, J., Hao, T., Nicot, A. S., Hirozane-Kishikawa, T., Vandenhaute, J., Orkin, S. H., Hill, D. E., van den Heuvel, S., and Vidal, M. (2004) Toward improving *Caenorhabditis elegans* phenome mapping with an ORFeome-based RNAi library. *Genome Res.* **14**, 2162–2168
63. Cotruvo, J. A., Jr., Aron, A. T., Ramos-Torres, K. M., and Chang, C. J. (2015) Synthetic fluorescent probes for studying copper in biological systems. *Chem. Soc. Rev.* **44**, 4400–4414
64. McWilliam, H., Li, W., Uludag, M., Squizzato, S., Park, Y. M., Buso, N., Cowley, A. P., and Lopez, R. (2013) Analysis tool web services from the EMBL-EBI. *Nucleic Acids Res.* **41**, W597–W600